BRAIN RESEARCH 1303 (2009) 195–206

available at www.sciencedirect.com

ScienceDirect

www.elsevier.com/locate/brainres

BRAIN RESEARCH

Research Report

Abnormal resting-state functional connectivity patterns of the putamen in medication-naïve children with attention deficit hyperactivity disorder

Xiaohua Cao[a,b], *Qingjiu Cao*[a,b], *Xiangyu Long*[c], *Li Sun*[a,b], *Manqiu Sui*[a,b], *Chaozhe Zhu*[c], *Xinian Zuo*[c], *Yufeng Zang*[c,*], *Yufeng Wang*[a,b,*]

[a]*Institute of Mental Health, Peking University, Beijing 100191, China*
[b]*Key Laboratory of Mental Health, Ministry of Health, Peking University, China*
[c]*State Key Laboratory of Cognitive Neuroscience and Learning, Beijing Normal University, Beijing 100875, China*

ARTICLE INFO

Article history:
Accepted 10 August 2009
Available online 20 August 2009

Keywords:
Attention deficit hyperactivity disorder
Functional magnetic resonance imaging
Resting state
Functional connectivity
Putamen

ABSTRACT

Structural and functional alterations of the putamen have been reported in patients with attention deficit hyperactivity disorder (ADHD), but the functional relationships between this area and other brain regions are seldom explored. In the present study, seed-based correlation analyses were performed in the resting-state functional magnetic resonance imaging (fMRI) data to examine the differences in functional connectivity of the putamen between medication-naïve children with ADHD and normal children. Positive functional connectivity with the putamen-ROIs was seen in bilateral sensorimotor area, prefrontal cortex, insula, superior temporal gyrus and subcortical regions and negative functional connectivity was located in bilateral parietal and occipital cortex as well as clusters in the frontal, middle temporal cortex and cerebellum. Group comparison showed that decreases in functional connectivity with the putamen-ROIs were observed in ADHD relative to the controls, except for the right globus pallidus/thalamus, which showed increased positive connectivity with left putamen-ROI. For children with ADHD, areas exhibiting decreased positive functional connectivity with left putamen-ROI were seen in right frontal and limbic regions, and regions showing decreased negative connectivity with the putamen-ROIs were observed in areas belonging to the default mode network (for left putamen-ROI, including right cerebellum and right temporal lobe; for right putamen-ROI, including left cerebellum and right precuneus). The above results suggest that abnormal functional relationships between the putamen and the cortical–striatal–thalamic circuits as well as the default mode network may underlie the pathological basis of ADHD.

1. Introduction

Attention deficit hyperactivity disorder (ADHD) is a prevalent childhood behavioral disorder with the core symptoms of inattention, hyperactivity and impulsivity. Convergent evidence has indicated that ADHD may be caused by abnormalities of frontal–striatal–cerebellar circuits (Valera et al., 2007; Bush et al., 2005).

* *Corresponding authors.* Y. Wang is to be contacted at Institute of Mental Health, Peking University, Huayuanbeilu 51, Haidian District, Beijing 100191, China. Fax: +86 10 6202 7314. Y. Zang, State Key Laboratory of Cognitive Neuroscience and Learning, Beijing Normal University, Beijing 100875, China.
E-mail addresses: zangyf@bnu.edu.cn (Y. Zang), wangyf@bjmu.edu.cn (Y. Wang).

0006-8993/$ – see front matter
doi:10.1016/j.brainres.2009.08.029

The striatum has been implicated in a number of discrete, distributed cortical–striatal–thalamic circuits involved in specific motor or cognitive functions (Alexander et al., 1986; Lawrence et al., 1998; Nakano et al., 2000). As an important structure of the striatum, the putamen has anatomical connection with cortical motor areas and is involved in high-level cognitive functions such as working memory (Chang et al., 2007) and language processing (Booth et al., 2007). There has been much evidence indicating abnormality of the putamen in ADHD. For example, human lesion studies suggested that dysfunction of the putamen was associated with symptoms of ADHD (Herskovits et al., 1999; Max et al., 2002). Additionally, several structural imaging studies reported reduced volume of the right putamen (Overmeyer et al., 2001; Wang et al., 2007) or reversal of asymmetry (Wellington et al., 2006) in the putamen in patients with ADHD. However, some investigators did not detect volumetric difference between ADHD and normal subjects (Castellanos et al., 1996; Aylward et al., 1996). As for functional imaging researches, Teicher et al. (2000) found that blood flow to bilateral putamen decreased in boys with ADHD. Cho et al. (2007) reported that in children with ADHD, resting-state regional cerebral blood flow (rCBF) in the putamen was associated with clinical response to methylphenidate, with higher rCBF in right putamen in non-responders relative to the responders. Besides, task-related functional imaging studies of ADHD revealed altered activation of the putamen in cognitive tasks in the patient group (Vaidya et al., 1998; Konrad et al., 2006; Cao et al., 2008). The above studies indicated that structural and functional abnormality of the putamen may play an important role in the pathology of ADHD.

Different regions in the brain do not act separately, and the integration of distinct brain areas was considered to be an important concept in the field of functional imaging research (Friston, 1994). Though previous studies suggest that structural and functional alterations of the putamen may contribute to the pathology of ADHD, little is known about the functional relationships between the putamen and other regions. The method of functional connectivity may answer this question to some extent.

Functional connectivity refers to temporal correlations between remote brain regions (Friston, 1994). Using this method, researchers have found that low-frequency (<0.08 Hz) fluctuations of resting-state blood oxygenation level-dependent (BOLD) signals were highly synchronous among motor, auditory, visual cortices and the language system in normal subjects (Biswal et al., 1995; Lowe et al., 1998; Cordes et al., 2001; Hampson et al., 2002).

Using functional magnetic resonance imaging (fMRI), Di Martino et al. (2008) mapped the resting-state functional connectivity of the striatum in 35 normal subjects, which provided evidence about functional organization of the basal ganglia consistent with previous theoretical models. It will be an interesting issue to investigate resting-state functional connectivity patterns of the striatum in patients with ADHD.

Up to now, there have been only a few studies exploring the functional connectivity features of ADHD, all of which are resting-state studies. In these published work, the researchers all selected the region of interest (ROI) located in the cortical areas, such as the dorsal anterior cingulate cortex (dACC) (Tian et al., 2006) and components of the default mode network (Castellanos et al., 2008; Uddin et al., 2008), a network consists of regions usually exhibiting task-related deactivations during performance of cognitive tasks (Raichle et al., 2001).

In this study, we used a seed-based correlation analysis to explore resting-state functional connectivity patterns of the putamen in children with and without ADHD. Because there has been evidence suggesting that methylphenidate administration may influence the regional blood flow or activation level in the putamen (Teicher et al., 2000; Vaidya et al., 1998), we only included the stimulant-naïve patients with ADHD in our study. Given the anatomical and functional characters of the putamen as well as results from previous imaging studies in ADHD, we hypothesized that alterations in functional connectivity patterns may be found in regions of the cortical–striatal–thalamic circuits in ADHD.

2. Results

2.1. Demographic data

The two groups were comparable in age. However, the children with ADHD had significantly lower IQ than the controls ($P = 0.005$). The patients showed significantly higher scores in the total score of ADHD RS-IV and its subscales ($P < 0.001$). The demographic and clinical characters of the subjects were summarized in Table 1.

2.2. Functional MRI results

2.2.1. Functional connectivity pattern of the putamen

Within-group functional connectivity patterns were revealed by one-sample *t*-tests in the ADHD group and control group, respectively (Fig. 1). In the control group, some regions showed positive functional connectivity with left and right putamen-ROIs, including bilateral putamen, caudate, globus pallidus, thalamus, insula (Brodmann area [BA] 13), bilateral inferior frontal gyrus (BA 47), ACC (BA 24, 32), medial frontal gyrus (BA 6), precentral gyrus (BA 6), postcentral gyrus (BA 2, 3), supramarginal gyrus (BA 40), superior temporal gyrus (BA 22) and some clusters in bilateral cerebellum. Negative functional connectivity

Table 1 – Demographic and clinical variables for controls and children with ADHD.

Variable	ADHD ($n = 19$) Mean (SD)	Controls ($n = 23$) Mean (SD)	*t*-value	*p*-value
Age	13.3 (1.4)	13.2 (1.0)	0.22	0.827
Full scale IQ	102.7 (10.4)	113.5 (11.4)	−2.976	0.005
ADHD RS-IV				
Total score	50.3 (9.2)	28.3 (6.1)	8.972	<0.001
Inattention	27.7 (4.3)	15.9 (4.6)	8.573	<0.001
Hyperactivity/impulsivity	22.6 (6.4)	12.4 (2.1)	7.315	<0.001

ADHD: attention deficit hyperactivity disorder. ADHD RS-IV: ADHD Rating Scale-IV.

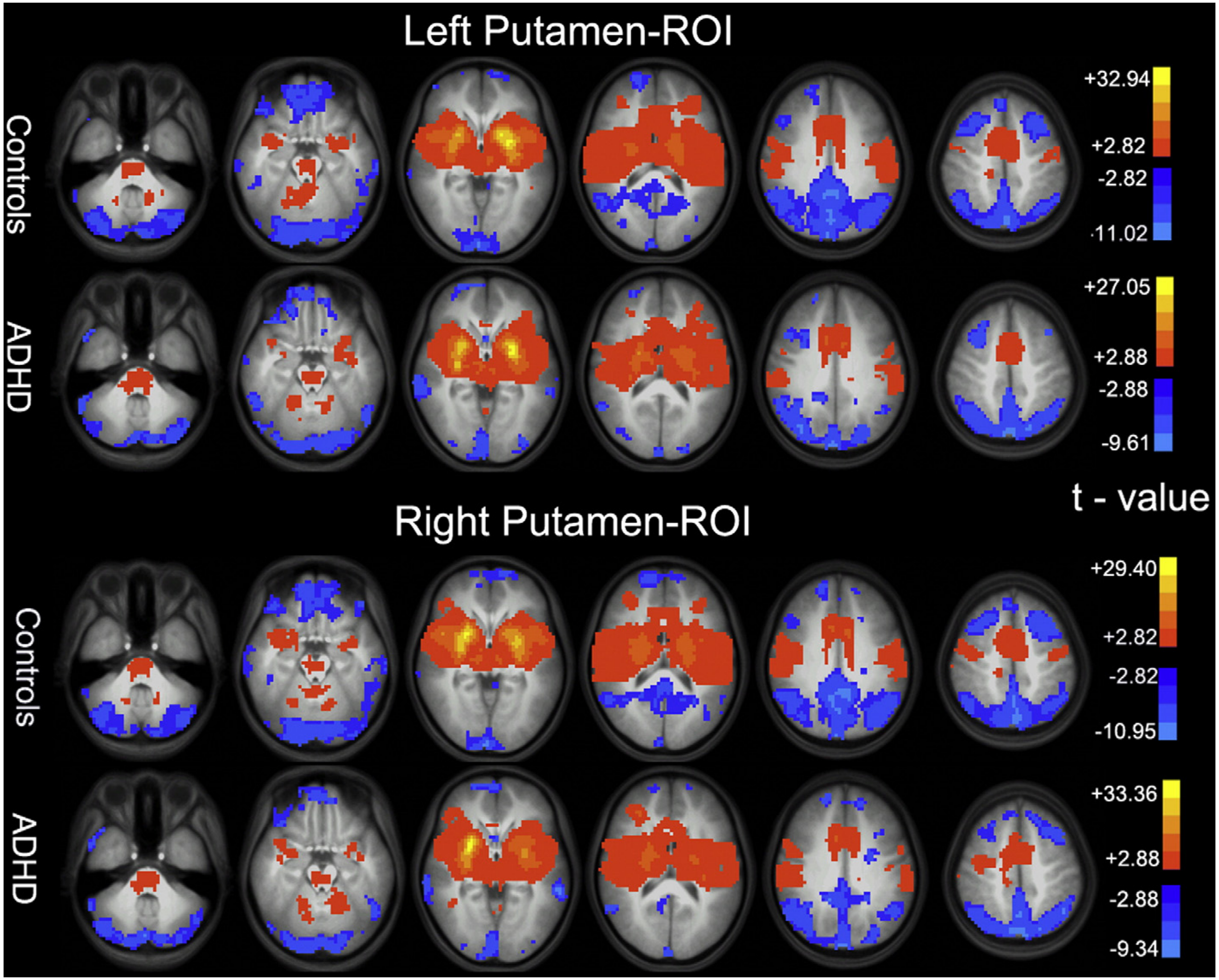

Fig. 1 – Patterns of significant positive (red) and negative (blue) functional connectivity with the putamen-ROIs in the controls and the ADHD group. Threshold was set at $P<0.05$ (corrected). In each row, the z coordinates of Talairach of the images were from $z=-32$ to $z=48$ mm (every 16 mm). Left in the figure indicates the right side of the brain. ADHD, attention deficit hyperactivity disorder. ROI: region of interest.

with the putamen-ROIs in the controls was evident in some areas including bilateral posterior cingulate cortex (PCC, BA 30, 31), precuneus (BA 7), angular gyrus (BA 39), superior parietal lobule (BA 7), cuneus (BA 19), bilateral middle/superior frontal gyrus (BA 6, 8), orbital gyrus (BA 11), middle temporal gyrus (BA 20, 21) and clusters in bilateral cerebellum. On the whole, the functional connectivity patterns of the ADHD group were roughly similar to that of the controls.

2.2.2. *Between-group differences of the functional connectivity pattern of the putamen*

Two-sample *t*-tests were performed to investigate the differences of functional connectivity of the putamen-ROIs between the two groups (Fig. 2 and Table 2). For the left putamen-ROI, regions demonstrating significant difference between the two groups involved right declive of the cerebellum, right superior temporal gyrus extending to right middle temporal gyrus (BA 22), right globus pallidus extending to right thalamus, right superior frontal gyrus (BA 6), and a cluster located in the limbic system, including right subcallosal gyrus and right nucleus accumbens. For the right putamen-ROI, areas showing significant difference in functional connectivity included right precuneus (BA 7) and left declive.

For each peak voxel that showed the greatest group difference within a specific brain area, the corresponding *t*-values in the four *t*-maps of one-sample *t*-tests (two for each group) were obtained. Positive *t* value means positive functional connectivity with the ROI and vice versa (See Table 2). It was found that most of the peak voxels did not show significant correlations with the putamen-ROIs in the ADHD group but showed significant positive or negative correlations in the control group. It means that, for most of these areas showing significant difference between the two groups, ADHD subjects exhibited decreased positive or negative connectivity with the putamen-ROIs. The right globus pallidus/thalamus was the only area which showed positive correlation with left putamen-ROI in both groups, with the ADHD group exhibiting significant increased functional connectivity relative to the controls. In summary, for the left putamen-ROI, increases in positive connectivity in ADHD were seen in right globus pallidus/thalamus, decreases in positive connectivity in ADHD were seen in the right subcallosal gyrus/nucleus accumbens and right superior frontal gyrus, and decreases in negative connectivity in ADHD were seen in the right declive and right superior/middle temporal gyrus. For the right putamen-ROI, decreases in negative connectivity in ADHD were observed in the right precuneus and left declive.

2.2.3. *Correlation between the symptoms and the strength of functional connectivity*

Correlation analysis was performed between the connectivity strength (i.e., mean z-values) and behavioral measures when IQ was taken as a covariate. The strength of functional connectivity of the left putamen-ROI to right subcallosal gyrus/nucleus accumbens showed significant negative correlation with the total score of ADHD RS-IV ($r=-0.667$, $P=0.002$) as well as with its two subscales (subscale of inattention: $r=-0.633$, $P=0.005$; subscale of hyperactivity/impulsivity: $r=-0.529$, $P=0.024$). The strength of functional connectivity of the left putamen-ROI to right globus pallidus/thalamus showed significant positive correlation with the total score of ADHD RS-IV ($r=0.510$, $P=0.03$). Analyses of other correlations did not show significant effects.

3. Discussion

In the present study, we explored the resting-state functional connectivity pattern of the putamen in ADHD. In the control group, a positive functional connectivity with the putamen-ROIs was seen in the bilateral sensorimotor area, prefrontal cortex, insula, superior temporal gyrus and subcortical regions while a negative functional connectivity was observed in areas of the parietal and occipital cortex as well as areas in the frontal, middle temporal cortex and the cerebellum. As for results of between-group analysis, regions showing group differences were distributed in the frontal (superior frontal gyrus), temporal (superior/middle temporal gyrus), parietal cortex (precuneus), subcortical area (subcallosal gyrus/nucleus accumbens, globus pallidus/thalamus) and the cerebellum. Except for the right globus pallidus/thalamus which showed increased positive functional connectivity with the left putamen-ROI in ADHD, other regions demonstrated significantly decreased functional connectivity with the putamen-ROIs in the patient group.

In the control group, a positive functional connectivity with the putamen-ROIs was seen in areas of the cortical–striatal–thalamic circuits, including the globus pallidus, thalamus, sensorimotor area (precentral gyrus and postcentral gyrus) and ACC. Previous researches have implicated anatomical connections of the putamen with a wide range of brain areas in the cortical–striatal–thalamic loops. Anatomical studies of the basal ganglia in primates confirmed the existence of the cortical–striatal–thalamic loops involving the sensorimotor area, supplementary motor area, premotor area, cingulate motor area, putamen, globus pallidus and thalamus (See review by Nakano et al., 2000). Additionally, two recent human studies using the diffuse tensor imaging (DTI) technique (Lehéricy et al., 2004a; Leh et al., 2007) revealed fiber connections between the putamen and a variety of areas including the prefrontal cortex, sensorimotor area, thalamus and cerebellum. In a meta-analysis of 126 functional imaging studies involving activation of the striatum in healthy participants (Postuma and Dagher, 2006), functional connectivity was defined as coactivation with the striatal nuclei. This meta-analysis provided evidence about functional connections of the basal ganglia. The only resting-state fMRI study investigating functional connectivity pattern of the striatum in normal adults was performed by Di Martino et al. (2008). In our study, a positive functional connectivity with the putamen-ROIs observed in the prefrontal cortex, caudate, insula, inferior parietal lobule, superior temporal gyrus and cerebellum was consistent with the findings of Postuma and Dagher (2006) and Di Martino et al. (2008). And the negative functional connectivity seen in the PCC, precuneus, angular gyrus and superior parietal lobule was also in accordance with the findings from Di Martino et al. (2008). The above results suggest widely spread functional connections of the putamen with cortical and subcortical areas in the brain. Positive functional connectivity was considered to serve an integrative role in combining neuronal activity subserving similar goals or representations (Fox et al., 2005). Similar to previous work

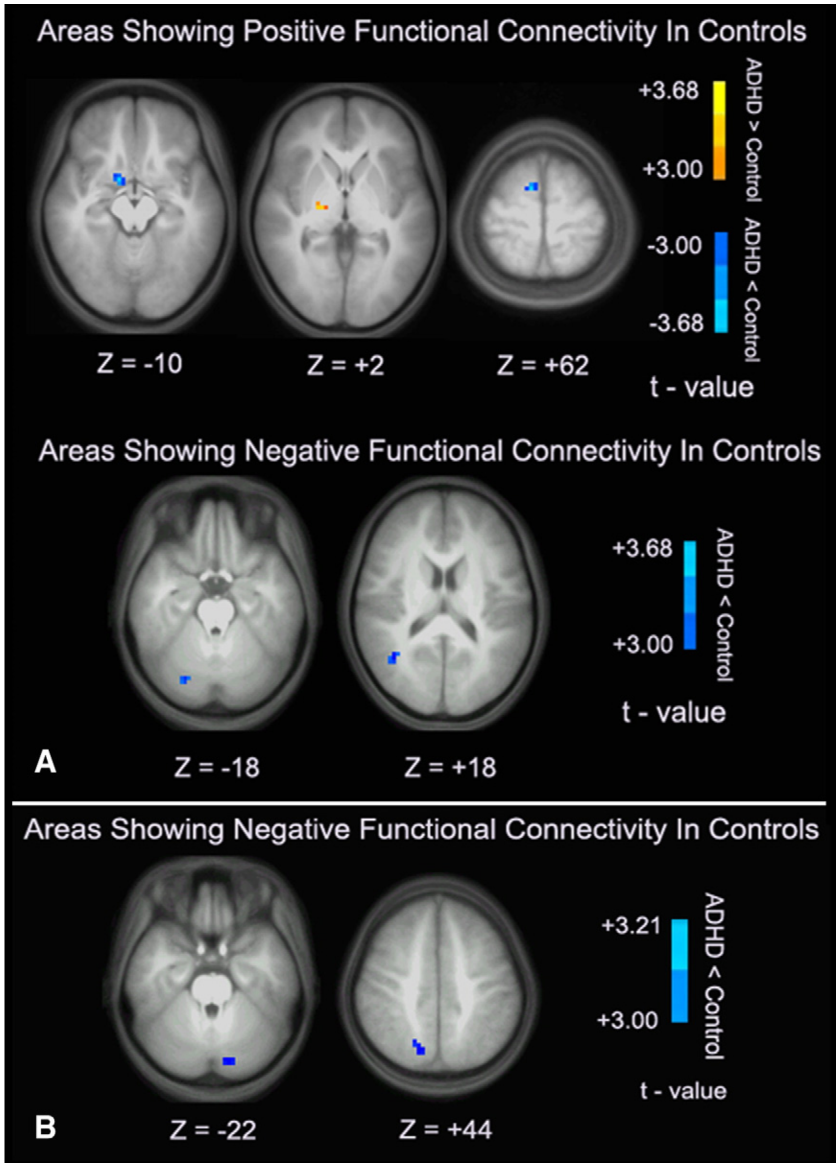

Fig. 2 – Regions showing differences in functional connectivity with the putamen-ROIs between groups. (A) Functional connectivity difference of left putamen-ROI. The upper row includes regions (from left to right: right subcallosal gyrus/nucleus accumbens, right globus pallidus extending to right thalamus, right superior frontal gyrus) exhibiting positive functional connectivity with left putamen-ROI in normal subjects, with the exception that right globus pallidus/thalamus also showed positive functional connectivity with left putamen-ROI in the ADHD group. The lower row includes regions (from left to right: right declive, right superior temporal gyrus extending to right middle temporal gyrus) exhibiting negative functional connectivity with left putamen-ROI in normal subjects. (B) Functional connectivity difference of right putamen-ROI. Fig. 3B includes regions (from left to right: left declive, right precuneus) exhibiting negative functional connectivity with right putamen-ROI in the control group. The numbers beneath each image refer to the *z* coordinates of Talairach and Tournoux. Threshold was set at $P<0.05$ (corrected). Left in the figure indicates the right side of the brain.

exploring functional connections of the striatum, our findings about positive functional connectivity pattern of the putamen-ROIs suggest existence of the functional circuit of the putamen. The nature of negative functional connectivity remains unclear. It has been proposed that regions belonging to antiphase networks (i.e., showing negative functional connectivity with each other) may subserve opposing or competitive processes (Greicius et al., 2003; Fox et al., 2005; Kelly et al., 2008), and negative correlations may reflect antagonistic influences of one network on another (Di Martino et al. 2008). Further work is needed to clarify characteristics of the anticorrelated network of the putamen.

It should be noted that the participants of the present study were children and adolescents aged from 11 to 16 years, while the subjects in the work of Di Martino et al. (2008) were healthy adults. Previous studies have investigated functional connectivity development of different brain regions in normal subjects (Fair et al., 2007, 2008; Kelly et al., 2009). In our study, functional

Table 2 – Regions showing difference in functional connectivity of the putamen-ROIs between groups.

Area	Functional connectivity pattern in each group*	Volume (mm^3)	BA	Side	Talairach (peak) x	y	z	t-value (peak)
Left putamen-ROI								
Areas showing positive functional connectivity in the controls								
ADHD>Control								
GP/Thal†	ADHD:+, Control: +	243		R	20	−14	2	3.372
ADHD<Control								
SclG/NAc	ADHD: 0, Control: +	351		R	10	4	−10	−3.602
SFG	ADHD: 0, Control: +	243	8	R	8	2	66	−3.678
Areas showing negative functional connectivity in the controls								
ADHD<Control								
Declive	ADHD: 0, Control: −	459		R	22	−70	−18	3.133
STG/MTG	ADHD: 0, Control: −	351	22	R	38	−56	18	3.288
Right putamen-ROI								
Areas showing negative functional connectivity in the controls								
ADHD<Control								
PCu	ADHD: 0, Control: −	513	7	R	14	−64	−44	3.110
Declive	ADHD: 0, Control: −	270		L	−14	−76	−22	3.209

*: For each peak voxel showing the greatest group difference within a specific brain area, the corresponding *t*-values in the four *t*-maps of one-sample *t*-tests (two for each group) were obtained. We used "+", "−" and "0" to signify significant positive, negative and no significant functional connectivity with the putamen-ROIs respectively. †: The right globus pallidus/thalamus also showed positive functional connectivity with left putamen-ROI in the ADHD group. GP/Thal: globus pallidus/thalamus. SclG/NAc: subcallosal gyrus/nucleus accumbens. SFG: superior frontal gyrus. STG/MTG: superior temporal gyrus/middle temporal gyrus. PCu: precuneus. BA: Brodmann area. ROI: region of interest. L, left; R, right. Threshold was set at $P<0.05$ (corrected). For positive functional connectivity, *t*-value > 0 (ADHD>Control) indicates that ADHD subjects showed significantly increased positive correlations with the putamen-ROIs compared with the controls and *t*-value < 0 (ADHD<Control) indicates the opposite. For negative functional connectivity, *t*-value > 0 (ADHD<Control) indicates that ADHD subjects showed significantly decreased negative correlations with the putamen-ROIs compared with the controls.

connectivity patterns of the putamen-ROIs have some similarities to the results of Di Martino et al. (2008). However, because we did not make comparison directly between children and adults, it is still unknown to what extent the similarities are. Further research about the development trajectory of functional connectivity in the putamen is merited.

In the patient group, increased positive functional connectivity relative to the controls was seen in the functional connectivity map of the left putamen-ROI, and the right globus pallidus/thalamus was the only area showing increased positive correlations with the left putamen-ROI in ADHD. The thalamus is a relay centre subserving both sensory and motor mechanisms (Herrero et al., 2002). Additionally, the putamen, globus pallidus and thalamus were all considered to be components of the basal ganglia circuit involved in motor function (Alexander et al., 1986; Lawrence et al., 1998). There has been evidence indicating structural or functional abnormality of the globus pallidus and thalamus in ADHD. For example, reduced volume of right globus pallidus has been reported in ADHD (Aylward et al., 1996; Castellanos et al., 1996; Overmeyer et al., 2001; Ellison-Wright et al., 2008), and enhanced resting-state activity of the thalamus was found in children with ADHD (Tian et al., 2008). We suppose that the abnormally increased functional connectivity of the putamen to the globus pallidus and thalamus may be due to dysfunction of the basal ganglia circuit involved in motor function, and may reflect compensatory recruitment of this circuit, which was in accordance with the hyperactivity symptom in ADHD.

For the left putamen-ROI, decreases in positive connectivity in ADHD were seen in right subcallosal gyrus/nucleus accumbens and right superior frontal gyrus. Connection between the nucleus accumbens and putamen has been found in animal studies (Russell, 2000), and functional connectivity between the putamen and areas in the prefrontal cortex such as the superior frontal gyrus has also been reported (Di Martino et al., 2008). The limbic system was implicated in the motivation-based dysfunction model of ADHD (Sonuga-Barke, 2005), in which the frontoventral striatal reward circuits (particularly the nucleus accumbens) were considered to be the neural basis. For example, animal studies showed that damage to the nucleus accumbens core caused rats to exhibit impulsive choice (Cardinal et al., 2004). The superior frontal gyrus was found to show reduced gray matter volume (Overmeyer et al., 2001) and decreased activation level in alerting (Cao et al., 2008) and response inhibition (Booth et al., 2005) tasks in children with ADHD. What's more, structural and functional disruptions of the superior frontal gyrus were found to coexist with abnormality of the putamen in ADHD (Overmeyer et al., 2001; Cao et al., 2008). In our study, decreased positive functional connectivity of the putamen-ROI to the nucleus accumbens and superior frontal gyrus in the patient group may indicate hypofunction of the frontoventral striatal and frontodorsal striatal circuits in ADHD, in accordance with the dual pathway model (Sonuga-Barke, 2005). According to this model, dysfunction of frontoventral striatal circuit may cause disrupted signaling of delayed reward, which is supported by the findings that children with ADHD often have difficulties in waiting and cannot work effectively over extended periods of time. While dysfunction of the frontodorsal striatal circuit may lead to impairments in executive functions such as inhibition control and attention, which is consistent with the impulsivity behaviors and inattention symptom in ADHD.

As for negative functional connectivity with the putamen-ROIs, only decreased negative connectivity was observed in the patient group as compared with the controls. For the left putamen-ROI, regions showing decreased negative connectivity in ADHD included the right declive of the cerebellum and right superior/middle temporal gyrus. For the right putamen-ROI, regions showing decreased negative connectivity in ADHD included the right precuneus and left declive. Previous imaging studies has reported smaller volume or hypoactivation of the cerebellum (Castellanos et al., 2002; Lee et al., 2005; Durston et al., 2004), precuneus (Carmona et al., 2005; Rubia et al., 2005) and temporal lobe (Carmona et al., 2005; Tamm et al., 2004) in ADHD. Additionally, the cerebellum, precuneus and middle temporal cortex were all considered to belong to the task-negative/default mode network (Fransson, 2005; Fox et al., 2005). Resting-state studies have found decreased negative functional connectivity between the ACC and regions in the default mode network in ADHD (Castellanos et al., 2008). Together with our results, components of the default mode network have been observed to show decreased negative functional connectivity with both cortical (ACC) and subcortical (putamen) regions in ADHD. The interference of the default mode network and attentional network has been suggested to be a potential underlying mechanism of performance variability in ADHD (Sonuga-Barke and Castellanos, 2007). Given its antiphase relationship with the task-positive networks which is engaged during attentionally demanding conditions (Fox et al., 2005), the default mode network may be involved in the neural basis of attentional dysfunction and is likely to be a candidate for attentional dysregulation in ADHD. As has been mentioned, negative functional connectivity may indicate antagonistic effect of one network on another (Di Martino et al., 2008). We supposed that decreased negative functional connectivity found in patients with ADHD may reflect impairment of the balance between the default mode network and other regions in the brain, and may be associated with the attentional disturbance of ADHD.

In our study, results of the exploratory correlation analysis linked functional connections of the putamen-ROIs to symptom severity of ADHD. The more abnormal functional connectivity patterns of the putamen-ROIs (i.e., more decreased functional connectivity in the subcallosal gyrus/nucleus accumbens and more increased connectivity in the globus pallidus/thalamus) were found in the patients, the more serious ADHD symptoms were. As mentioned above, the nucleus accumbens, globus pallidus and thalamus were all components of the cortical–striatal–thalamic circuits (Alexander et al., 1986) and related to neurobiological basis of ADHD. The quantitative relationship between symptom severity of ADHD and strength of the functional connectivity of the nucleus accumbens, globus pallidus and thalamus with the putamen-ROIs indicates the vital role of the basal ganglia loops in the pathophysiology of ADHD.

In the present study, regions showing group difference in functional connectivity with the left putamen-ROIs did not overlapped the regions showing group difference in functional connectivity with the right putamen-ROI. This inconsistency may result from the intrinsic functional difference between left and right putamen or from different volumes of the two putamen-ROIs defined in our study. Further studies on the asymmetry of functional connectivity of putamen are needed.

It should be noted that most of the regions showing group difference in functional connectivity with the putamen-ROIs were located contralaterally to the corresponding seed region. Contralateral anatomical connections between the putamen and cortical areas were described in a DTI study in healthy subjects (Lehéricy et al., 2004b). Additionally, resting-state fMRI studies (Postuma and Dagher, 2006; Di Martino et al., 2008) demonstrated that most of the regions exhibiting functional connectivity with the putamen were located bilaterally or in the contralateral side of the seed region. It is not clear why abnormal functional connections of the putamen in ADHD existed mainly in the contralateral side of the seed region. A recent electroencephalography study revealed altered functional connectivity between frontal and contralateral cortical areas in children with ADHD, which may “reflect differences in functional callosal connections between the 2 groups” (Murias et al., 2007). In other words, the authors considered that abnormal interhemispheric functional connectivity may be associated with abnormality in fibers tracts connecting the two hemispheres. Hence the altered functional connectivity between the putamen and contralateral regions may be due to disturbance in white matter tracts connecting the putamen and regions in its contralateral side. Further work combining DTI and fMRI is needed to clarify the relationship between anatomical connections and functional connectivity, which is helpful to make clear whether disrupted contralateral connectivity is associated with abnormal anatomical connections.

Several limitations should be noted in the present study. Firstly, the AAL template was used as the basis of the seed regions in our study, i.e., the same ROI size was used for each subject regardless of the individual variability of the putamen volume. An alternative method is to define subject-specific putamen-ROIs by manual drawing. However, manual drawing is labor intensive and somewhat subjective. In future work, more refined and optimized method should be produced for the definition of seed ROIs. Secondly, the patient group showed lower IQ than the controls. The relationship between IQ and resting-state brain activity remains unclear. Thirdly, two subtypes were recruited in the ADHD group in the current study, and the comorbidity condition in the patients may have confounding effect. Future studies with large sample size could compare between subtypes. Finally, an issue of the scanning parameters of the structural data should be addressed. In the current study, the structural images of the participants were used in the process of registration (see the section of Experimental procedures), which is believed to improve the spatial normalization (Ashburner and Friston, 2005). Our data were collected in a period of about two years and some modifications were made in the sequences of structural images. Totally, there were four kinds of parameters. As can be seen in Image acquisition, two kinds of the parameters were used in most (40 of 42) of the participants. These two main sequences almost have similar distribution across the two groups and they may have similar effect on the two groups. It is likely that the difference in scanning parameters may not influence the results of spatial normalization significantly. However, we cannot exclude the potential effect of these variations of scanning parameters on the results.

In summary, we found decreased functional connectivity of the putamen-ROIs in ADHD, with the right frontal and limbic regions showing decreased positive functional connectivity and areas in the default mode network showing decreased negative functional connectivity. The right globus pallidus/thalamus showed increased positive connectivity with left putamen-ROI. And the strength of functional connectivity is correlated with symptom severity of ADHD. The above results indicate abnormal relationships between the putamen and distributed regions located in the cortical–striatal–thalamic circuits and the default mode network in ADHD.

4. Experimental procedures

4.1. *Subjects*

Subjects of the current study included 23 stimulant-naïve boys diagnosed with ADHD and 25 age-matched healthy male controls. The data used in the present study were part of the dataset analyzed by Cao et al. (2006). In the work of Cao et al. (2006), some patients with a history of stimulant medication were also included. Details of the participants in our study as well as the relationship between the subjects of our study and those of the study by Cao et al. (2006) were listed in Table 3.

All participants were between 11 and 16 years. All of the subjects met the following criteria: 1) right-handedness; 2) no lifetime history of head trauma with loss of consciousness; 3) no history of neurological illness or other severe diseases; 4) no history of psychiatric disorders including schizophrenia, affective disorders, anxiety, Tourette disorder, pervasive developmental disorder and mental retardation except for ADHD diagnosis in the patient group; 5) full scale IQ higher than 80 measured by the Wechsler Intelligence Scale for Chinese Children-Revised (WISCC-R) (Gong and Cai, 1993); 6) no previous treatment with stimulants. Patients with comorbid oppositional defiant disorder (ODD) or conduct disorder (CD) were not excluded.

The patients were recruited from the outpatients of Institute of Mental Health, Peking University. ADHD diagnosis was determined via a structured diagnostic interview, the Clinical Diagnostic Interviewing Scale (CDIS) (Yang et al., 2001), which is based on DSM-IV criteria. Boys in the control group were recruited from schools nearby. Their parents were interviewed with CDIS to ensure that they were excluded from diagnosis of ADHD. For all the participants, scores of the ADHD Rating Scale-IV (ADHD RS-IV) (DuPaul et al., 1998) were reported by the parents. The ADHD RS-IV contains 18 items corresponding to the DSM-IV criteria for ADHD. Each symptom is scored according to how often it occurred (i.e., "never" is rated as 1, "occasionally" is 2; "often" is 3; "always" is 4).

Data from 4 patients and 2 normal subjects were excluded due to excessive head motion during fMRI acquisition (see Data analysis). Hence there were 19 subjects in the ADHD group and 23 in the control group. Additionally, seven of the 19 patients met the criteria for the combined type and the other 12 met the criteria for the predominantly inattentive type. Five patients had comorbid ODD and 2 had comorbid CD.

This study was approved by the Research Ethics Review Board of Institute of Mental Health, Peking University. After a complete description of the study procedures, written informed consent was obtained from parents or guardians of the subjects and all of the children agreed to participate.

Table 3 – Composition of the participants.

	ADHD	Controls
Number of subjects in the study by Cao et al. (2006)	29	27
Number of subjects excluded from the study by Cao et al. (2006)	6	2
History of medication treatment	6	0
Poor quality of structural image	0	2
Number of subjects included in the current study	23	25
Number of subjects excluded because of excessive head motion	4	2
Number of subjects included in the final analysis	19[a]	23

[a] : Among the 19 patients included in the statistical analysis, 5 patients had comorbid ODD and 2 had comorbid CD. ADHD: attention deficit hyperactivity disorder. ODD: oppositional defiant disorder. CD: conduct disorder.

4.2. *Image acquisition*

Images were acquired using a Siemens Trio 3-Tesla scanner (Siemens, Erlangen, Germany) in the Institute of Biophysics, Chinese Academy of Sciences. All of the resting-state functional data were acquired using an echo-planar imaging (EPI) sequence with the following parameters: 30 axial slices, repetition time (TR) = 2000 ms, echo time (TE) = 30 ms, flip angle = 90°, thickness/skip = 4.5/0 mm, field of view (FOV) = 220 × 220 mm, matrix = 64 × 64, 240 volumes.

For each subject, a high resolution T1-weighted anatomical image was acquired in a sagittal orientation using a spoiled gradient-recalled sequence covering the whole brain, which was used for the purpose of image registration and visualization (see Data analysis). Our data were collected in a period of about two years and some modifications were made in the sequence of the structural images. Among the 42 participants (19 ADHD and 23 controls) included in the statistical analysis, four kinds of parameters were involved. Most of the subjects (see details below) were scanned with one of the following two kinds of parameters: 1) 192 slices, TR = 2000 ms, TE = 3.67 ms, inversion time = 1100 ms, flip angle = 12°, FOV = 240 × 240 mm, matrix = 256 × 256, used in 8 patients and 12 controls; 2) 176 slices, TR = 1770 ms, TE = 3.92 ms, inversion time = 1100 ms, flip angle = 12°, FOV = 256 × 256 mm, matrix = 512 × 512, used in 9 patients and 11 controls. Additionally, another two kinds of parameters were used in two individuals respectively: 3) 128 slices, TR = 1950 ms, TE = 2.6 ms, inversion time = 900 ms, flip angle = 10°, FOV = 240 × 256 mm, matrix = 240 × 256, used in

1 patient; 4) 128 slices, TR = 2530 ms, TE = 3.37 ms, inversion time = 1100 ms, flip angle = 7°, FOV = 256 × 256 mm, matrix = 256 × 256, used in 1 patient.

Other scanning sessions, which have no relation to the present study, are not described here. Resting state was defined as no specific cognitive task during the fMRI scanning (Biswal et al., 1995). Participants were asked simply to remain still, close their eyes, think of nothing systematically and not fall asleep.

4.3. *Data analysis*

The first 10 volumes of each subject's functional time series were discarded for signal stabilization and for the subjects to get used to the scanner noise. Then the data were preprocessed using the SPM5 software package (http://www.fil.ion.ucl.ac.uk/spm). Firstly, slice timing and head motion correction were carried out. Excessive motion was defined as more than 3 mm of translation or more than 3 degrees of rotation in any direction. Data of 4 boys in the patient group and 2 in the control group were excluded from further analysis according to this criterion. The structural image of each subject was coregistered to the functional image after head motion correction. Then the coregistered structural images were segmented using the unified segmentation algorithm which could improve the accuracy of spatial normalization significantly (Ashburner and Friston, 2005) and then transformed into standard Montreal Neurological Institute (MNI) space. The functional images were also spatially normalized to MNI space by applying the parameters of structural image normalization and were resampled to a voxel size of $3 \times 3 \times 3$ mm^3. Subsequently, spatial smoothing was conducted with a Gaussian kernel of 4 mm full width at half maximum.

Further preprocessing was performed using a home-made software Resting-State fMRI Data Analysis Toolkit (REST, by Song et al., http://resting-fmri.sourceforge.net), including removal of linear trend and temporal band-pass filtering (0.01–0.08 Hz) to reduce low-frequency drift and high-frequency respiratory and cardiac noise.

The regions of interest (ROIs) of the putamen were defined according to the automated anatomical labeling (AAL) template (Tzourio-Mazoyer et al., 2002) in the MRIcro software (by Chris Rorden, http://www.sph.sc.edu/comd/rorden/mricro.html). In an attempt to make sure that the ROIs were located within the putamen for each subject and therefore to reduce the confounding effect from adjacent non-putamen signals, all the voxels ($1 \times 1 \times 1$ mm^3) in the outmost layer of the ROIs were removed, i.e., smaller putamen-ROIs were generated. The smaller putamen-ROIs were superimposed on individual spatial normalized 3D images and it was found that they did not exceed the boundary of the putamen in any subject. Then the putamen-ROIs were resampled to $3 \times 3 \times 3$ mm^3 for further analysis. Because the AAL template was generated from the MNI single-subject brain and was not symmetric in the two hemispheres, volumes of the two ROIs in our study based on the AAL template were also different, with a cluster of 169 voxels (4563 mm^3) in left putamen-ROI and a cluster of 184 voxels (4968 mm^3) in right putamen-ROI after resampling (Fig. 3). Subsequent processes were done in left and right putamen-ROIs separately.

At the individual level, the calculation of functional connectivity was carried out using the REST software. Firstly, three nuisance covariates, i.e., global trend, white matter (WM) and cerebrospinal fluid (CSF), were obtained by averaging the time series within the whole brain, WM and CSF masks respectively, which were contained in the REST software. For each of the putamen-ROIs, a seed reference time course was obtained by averaging the time series of all voxels in the ROI. Then Pearson's correlation analysis was performed between the seed reference time course and time series of each voxel in the brain in a voxel-wise way, with the global signal, WM signal, CSF signal and the 6 head motion parameters as nuisance covariates. The resultant correlation coefficients were transformed into z-scores using Fisher's transformation so that their distribution could better satisfy normality (Press et al., 1992).

4.4. *Statistics*

As for the imaging data, statistic analyses were performed using AFNI software (Analysis of Functional NeuroImages, http://afni.nimh.nih.gov/). Firstly, random-effect one-sample t-tests were conducted on the individual z-maps of the two groups separately, producing four t-maps corresponding to the functional connectivity patterns of left and right putamen-ROIs in both groups. The four t-maps were superimposed on the mean normalized structural images of all subjects and then were transformed to Talairach and Tournoux coordinates (Talairach and Tournoux, 1988). The t-maps were masked by the global

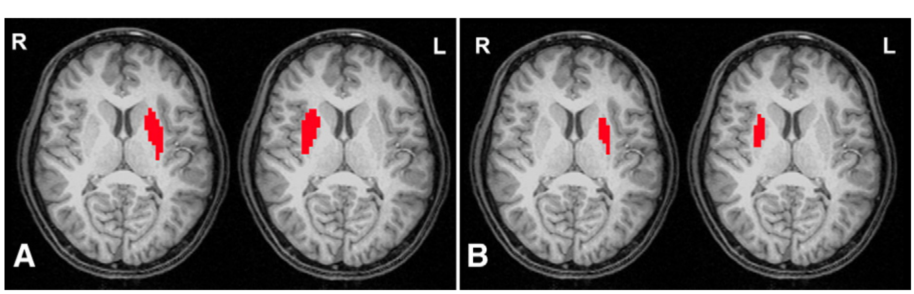

Fig. 3 – The regions of interest (ROIs) of left and right putamen, superimposed on the normalized structural image of one subject. The images were set at Talairach coordinate of z = 10 and the putamen-ROIs were showed with red color. (A) ROIs extracted from the AAL template, exceeding the boundary of the putamen in this subject. (B) After the outmost layer was removed, the ROIs were within the boundary of the putamen in the subject. L: left; R: right.

mask to include only voxels within the brain. Multiple comparisons correction was performed using the AlphaSim program written by B. Douglas Ward in the AFNI software determined by Monte Carlo simulations. And statistical maps of one-sample *t*-tests were set at a combined threshold of $P<0.01$ and a minimum cluster size of 270 mm^3 (10 voxels), yielding a corrected threshold of $P<0.05$.

Because the ADHD group had significant lower IQ scores than the controls ($P<0.005$, see Table 1), we carried out between-group analyses taking the potential effect of IQ into account. For each putamen-ROI, regression analysis was performed using the 3dRegAna program in AFNI with the IQ score and group (ADHD or controls) as regressors. The resultant *t*-maps represented the between-group difference when the IQ effect was controlled. Multiple comparisons correction for the results of between-group comparisons was constrained within two masks respectively, named *smaller-masks* temporally, corresponding to connectivity pattern of the left and right putamen-ROIs. The smaller-masks were generated from the results of one-sample *t*-tests. One smaller-mask included only the voxels showing significant functional connectivity with the left putamen-ROI in at least one group, and similarly the other smaller-mask contained only the voxels showing significant functional connectivity with the right putamen-ROI in at least one group. Multiple comparisons correction was done by using AlphaSim program in AFNI and a corrected threshold of $P<0.05$ was utilized, with a combined threshold of $P<0.01$ and a minimum cluster size of 243 mm^3 (9 voxels). Between-group results were superimposed on the mean normalized structural images of all subjects.

Finally, in order to investigate the relationship between the strength of functional connectivity and symptom severity, exploratory partial correlation analyses were done between the mean *z*-scores of each cluster showing significant group differences and the ADHD RS-IV scores in the ADHD group, with IQ as a controlled variable. A two-tailed *P* level of 0.05 was used as the criterion of statistical significance.

Acknowledgments

This work was supported in part by the National Natural Sciences Foundation of China (NSFC) (30770774, YFW), the Commonweal Sciences Foundation, Ministry of Health, China (200802073, YFW), the National Foundation, Ministry of Science and Technology, China (2007BAI17B03, YFW), the NSFC (30621130074, YFZ) and 863 program (2008AA02Z405, YFZ). We thank the individuals who served as research participants. The authors report no biomedical financial interests or potential conflicts of interest.

REFERENCES

Alexander, G.E., DeLong, M.R., Strick, P.L., 1986. Parallel organization of functionally segregated circuits linking basal ganglia and cortex. Annu. Rev. Neurosci. 9, 357–381.

Ashburner, J., Friston, K.J., 2005. Unified segmentation. NeuroImage 26, 839–851.

Aylward, E.H., Reiss, A.L., Reader, M.J., Singer, H.S., Brown, J.E., Denckla, M.B., 1996. Basal ganglia volumes in children with attention deficit hyperactivity disorder. J. Child Neurol. 11, 112–115.

Biswal, B., Yetkin, F.Z., Haughton, V.M., Hyde, J.S., 1995. Functional connectivity in the motor cortex of resting human brain using echo-planar MRI. Magn. Reson. Med. 34, 537–541.

Booth, J.R., Burman, D.D., Meyer, J.R., Lei, Z., Trommer, B.L., Davenport, N.D., Li, W., Parrish, T.B., Gitelman, D.R., Mesulam, M.M., 2005. Larger deficits in brain networks for response inhibition than for visual selective attention in attention deficit hyperactivity disorder (ADHD). J. Child Psychol. Psychiatry 46, 94–111.

Booth, J.R., Wood, L., Lu, D., Houk, J.C., Bitan, T., 2007. The role of the basal ganglia and cerebellum in language processing. Brain Res. 1133, 136–144.

Bush, G., Valera, E.M., Seidman, L.J., 2005. Functional neuroimaging of attention-deficit/hyperactivity disorder: a review and suggested future directions. Biol. Psychiatry 57, 1273–1284.

Cao, Q.J., Zang, Y.F., Sun, L., Sui, M.Q., Long, X.Y., Zou, Q.H., Wang, Y.F., 2006. Abnormal neural activity in children with attention deficit hyperactivity disorder: a resting-state functional magnetic resonance imaging study. NeuroReport 17, 1033–1036.

Cao, Q., Zang, Y., Zhu, C., Cao, X., Sun, L., Zhou, X., Wang, Y., 2008. Alerting deficits in children with attention deficit/hyperactivity disorder: event-related fMRI evidence. Brain Res. 1219, 159–168.

Cardinal, R.N., Winstanley, C.A., Robbins, T.W., Everitt, B.J., 2004. Limbic corticostriatal systems and delayed reinforcement. Ann. N. Y. Acad. Sci. 1021, 33–50.

Carmona, S., Vilarroya, O., Bielsa, A., Tremols, V., Soliva, J.C., Rovira, M., Tomas, J., Raheb, C., Gispert, J.D., Batlle, S., Bulbena, A., 2005. Global and regional gray matter reductions in ADHD: a voxel based morphometric study. Neurosci. Lett. 389, 88–93.

Castellanos, F.X., Giedd, J.N., Hamburger, S.D., Vaituzis, A.C., Dickstein, O.P., Sarfatti, S.E., Vauss, Y.C., Snell, J.W., Lange, N., Kaysen, D., Krain, A.L., Ritchie, G.F., Rajapakse, J.C., Rapoport, J.L., 1996. Quantitative brain magnetic resonance imaging in attention-deficit/hyperactivity disorder. Arch. Gen. Psychiatry 53, 607–616.

Castellanos, F.X., Lee, P.P., Sharp, W., Jeffries, N.O., Greenstein, D.K., Clasen, L.S., Blumenthal, J.D., James, R.S., Ebens, C.L., Walter, J.M., Zijdenbos, A., Evans, A.C., Giedd, J.N., Rapoport, J.L., 2002. Developmental trajectories of brain volume abnormalities in children and adolescents with attention-deficit/hyperactivity disorder. JAMA 288, 1740–1748.

Castellanos, F.X., Margulies, D.S., Kelly, C., Uddin, L.Q., Ghaffari, M., Kirsch, A., Shaw, D., Shehzad, Z., Di Martino, A., Biswal, B., Sonuga-Barke, E.J., Rotrosen, J., Adler, L.A., Milham, M.P., 2008. Cingulate–precuneus interactions: a new locus of dysfunction in adult attention-deficit/hyperactivity disorder. Biol. Psychiatry 63, 332–337.

Chang, C., Crottaz-Herbette, S., Menon, V., 2007. Temporal dynamics of basal ganglia response and connectivity during verbal working memory. NeuroImage 34, 1253–1269.

Cho, S.C., Hwang, J.W., Kim, B.N., Lee, H.Y., Kim, H.W., Lee, J.S., Shin, M.S., Lee, D.S., 2007. The relationship between regional cerebral blood flow and response to methylphenidate in children with attention-deficit hyperactivity disorder: comparison between non-responders to methylphenidate and responders. J. Psychiatr. Res. 41, 459–465.

Cordes, D., Haughton, V.M., Arfanakis, K., Carew, J.D., Turski, P.A., Moritz, C.H., Quigley, M.A., 2001. Frequencies contributing to functional connectivity in the cerebral cortex in "resting-state" data. Am. J. Neuroradiol. 22, 1326–1333.

Di Martino, A., Scheres, A., Margulies, D.S., Kelly, A.M., Uddin, L.Q., Shehzad, Z., Biswal, B., Walters, J.R., Castellanos, F.X., Milham, M.P., 2008. Functional connectivity of human striatum: a resting state fMRI study. Cereb. Cortex 18, 2735–2747.

DuPaul, G.J., Power, T.J., Anastopoulos, A.D., Reid, R., 1998. ADHD Rating Scale-IV: checklists, norms, and clinical interpretations. The Guilford Press, New York.
Durston, S., Hulshoff Pol., H.E., Schnack, H.G., Buitelaar, J.K., Steenhuis, M.P., Minderaa, R.B., Kahn, R.S., van Engeland, H., 2004. Magnetic resonance imaging of boys with attention-deficit/hyperactivity disorder and their unaffected siblings. J. Am. Acad. Child Adolesc. Psychiatry 43, 332–340.
Ellison-Wright, I., Ellison-Wright, Z., Bullmore, E., 2008. Structural brain change in ADHD identified by meta-analysis. BMC Psychiatry 8, 51.
Fair, D.A., Dosenbach, N.U.F., Church, J.A., Cohen, A.L., Brahmbhatt, S., Miezin, F.M., Barch, D.M., Raichle, M.E., Petersen, S.E., Schlaggar, B.L., 2007. Development of distinct control networks through segregation and integration. Proc. Natl Acad. Sci. U. S. A. 104, 13507–13512.
Fair, D.A., Cohen, A.L., Dosenbach, N.U.F., Church, J.A., Miezin, F.M., Barch, D.M., Raichle, M.E., Petersen, S.E., Schlaggar, B.L., 2008. The maturing architecture of the brain's default network. Proc. Natl Acad. Sci. U. S. A. 105, 4028–4032.
Fox, M.D., Snyder, A.Z., Vincent, J.L., Corbetta, M., Van Essen, D.C., Raichle, M.E., 2005. The human brain is intrinsically organized into dynamic, anticorrelated functional networks. Proc. Natl Acad. Sci. U. S. A. 102, 9673–9678.
Fransson, P., 2005. Spontaneous low-frequency BOLD signal fluctuations: an fMRI investigation of the resting-state default mode of brain function hypothesis. Hum. Brain Mapp. 26, 15–29.
Friston, K.J., 1994. Functional and effective connectivity in neuroimaging: a synthesis. Hum. Brain Mapp. 2, 56–78.
Gong, Y.X., Cai, T.S., 1993. Manual of Chinese Revised Wechsler Intelligence Scale for Children (In Chinese). Hunan Atlas Press, Changsha.
Greicius, M.D., Krasnow, B., Reiss, A.L., Menon, V., 2003. Functional connectivity in the resting brain: a network analysis of the default mode hypothesis. Proc. Natl Acad. Sci. U. S. A. 100, 253–258.
Hampson, M., Peterson, B.S., Skudlarski, P., Gatenby, J.C., Gore, J.C., 2002. Detection of functional connectivity using temporal correlations in MR images. Hum. Brain Mapp. 15, 247–262.
Herrero, M.T., Barcia, C., Navarro, J.M., 2002. Functional anatomy of thalamus and basal ganglia. Child's Nerv. Syst. 18, 386–404.
Herskovits, E.H., Megalooikonomou, V., Davatzikos, C., Chen, A., Bryan, R.N., Gerring, J.P., 1999. Is the spatial distribution of brain lesions associated with closed-head injury predictive of subsequent development of attention-deficit/hyperactivity disorder? Analysis with brain-image database. Radiology 213, 389–394.
Kelly, A.M.C., Uddin, L.Q., Biswal, B.B., Castellanos, F.X., Milham, M.P., 2008. Competition between functional brain networks mediates behavioral variability. Neuroimage 39, 527–537.
Kelly, A.M.C., Di Martino, A., Uddin, L.Q., Shehzad, Z., Gee, D.G., Reiss, P.T., Margulies, D.S., Castellanos, F.X., Milham, M.P., 2009. Development of anterior cingulate functional connectivity from late childhood to early adulthood. Cereb. Cortex 19, 640–657.
Konrad, K., Neufang, S., Hanisch, C., Fink, G.R., Herpertz-Dahlmann, B., 2006. Dysfunctional attentional networks in children with attention deficit/hyperactivity disorder: evidence from an event-related functional magnetic resonance imaging study. Biol. Psychiatry 59, 643–651.
Lawrence, A., Sahakian, B., Robbins, T., 1998. Cognitive functions and corticostratal circuits: insights from Huntington's disease. Trends Cogn. Sci. 2, 379–388.
Lee, J.S., Kim, B.N., Kang, E., Lee, D.S., Kim, Y.K., Chung, J.K., Lee, M.C., Cho, S.C., 2005. Regional cerebral blood flow in children with attention deficit hyperactivity disorder: comparison before and after methylphenidate treatment. Hum. Brain Mapp. 24, 157–164.
Leh, S.E., Ptito, A., Chakravarty, M.M., Strafella, A.P., 2007. Fronto-striatal connections in the human brain: a probabilistic diffusion tractography study. Neurosci. Lett. 419, 113–118.
Lehéricy, S., Ducros, M., Krainik, A., Francois, C., Van de Moortele, P.F., Ugurbil, K., Kim, D.S, 2004a. 3-D Diffusion tensor axonal tracking shows distinct SMA and Pre-SMA projections to the human striatum. Cereb. Cortex 14, 1302–1309.
Lehéricy, S., Ducros, M., Van de Moortele, P.F., Francois, C., Thivard, L., Poupon, C., Swindale, N., Ugurbil, K., Kim, D.S., 2004b. Diffusion tensor fiber tracking shows distinct corticostriatal circuits in humans. Ann. Neurol. 55, 522–529.
Lowe, M.J., Mock, B.J., Sorenson, J.A., 1998. Functional connectivity in single and multislice echoplanar imaging using resting-state fluctuations. NeuroImage 7, 119–132.
Max, J.E., Fox, P.T., Lancaster, J.L., Kochunov, P., Mathews, K., Manes, F.F., Robertson, B.A., Arndt, S., Robin, D.A., Lansing, A.E., 2002. Putamen lesions and the development of attention deficit/hyperactivity symptomatology. J. Am. Acad. Child Adolesc. Psychiatry 41, 563–571.
Murias, M., Swanson, J.M., Srinivasan, R., 2007. Functional connectivity of frontal cortex in healthy and ADHD children reflected in EEG coherence. Cereb. Cortex 17, 1788–1799.
Nakano, K., Kayahara, T., Tsutsumi, T., Ushiro, H., 2000. Neural circuits and functional organization of the striatum. J. Neurol. 247 (Suppl 5), V1–V15.
Overmeyer, S., Bullmore, E.T., Suckling, J., Simmons, A., Williams, S.C.R., Taylor, P.J., Santosh, E., 2001. Distributed grey and white matter deficits in hyperkinetic disorder: MRI evidence for anatomical abnormality in an attentional network. Psychol. Med. 31, 1425–1435.
Postuma, R.B., Dagher, A., 2006. Basal ganglia functional connectivity based on a meta-analysis of 126 positron emission tomography and functional magnetic resonance imaging publications. Cereb. Cortex 16, 1508–1521.
Press, W.H., Flannery, B.P., Teukolsky, S.A., Vetterling, W.T., 1992. Numerical Recipes in C, The Art of Scientific Computing, Second ed. Cambridge University Press, UK.
Raichle, M.E., MacLeod, A.M., Snyder, A.Z., Powers, W.J., Gusnard, D.A., Shulman, G.L., 2001. A default mode of brain function. Proc. Natl Acad. Sci. U. S. A. 98, 676–682.
Rubia, K., Smith, A.B., Brammer, M., Toone, B., Taylor, E., 2005. Abnormal brain activation during inhibition and error detection in medication-naïve adolescents with attention-deficit hyperactivity disorder. Am. J. Psychiatry 162, 1067–1075.
Russell, V.A., 2000. The nucleus accumbens motor-limbic interface of the spontaneously hypertensive rat as studied in vitro by the superfusion slice technique. Neurosci. Biobehav. Rev. 24, 133–136.
Sonuga-Barke, E.J.S., 2005. Causal models of attention-deficit/hyperactivity disorder: from common simple deficits to multiple developmental pathways. Biol. Psychiatry 57, 1231–1238.
Sonuga-Barke, E.J.S., Castellanos, F.X., 2007. Spontaneous attentional fluctuations in impaired states and pathological conditions: a neurobiological hypothesis. Neurosci. Biobehav. Rev. 31, 977–986.
Talairach, J., Tournoux, P., 1988. Coplanar Stereotactic Atlas of the Human Brain. Thieme, Stuttgart.
Tamm, L., Menon, V., Ringel, J., Reiss, A.L., 2004. Event-related fMRI evidence of frontotemporal involvement in aberrant response inhibition and task switching in attention-deficit/hyperactivity disorder. J. Am. Acad. Child Adolesc. Psychiatry 43, 1430–1440.
Teicher, M.H., Anderson, C.M., Glod, C.A., Maas, L.C., Renshaw, P.F., 2000. Functional deficits in basal ganglia of children with attention-deficit/hyperactivity disorder show with functional magnetic resonance imaging relaxomety. Nat. Med. 6, 470–474.

Tian, L.X., Jiang, T.Z., Liang, M., Zang, Y.F., He, Y., Sui, M.Q., Wang, Y.F., 2008. Enhanced resting-state brain activities in ADHD patients: a fMRI study. Brain Dev. 30, 342–348.

Tian, L.X., Jiang, T.Z., Wang, Y.F., Zang, Y.F., He, Y., Liang, M., Sui, M.Q., Cao, Q.J., Hu, S.Y., Peng, M., Zhuo, Y., 2006. Altered resting-state functional connectivity patterns of anterior cingulate cortex in adolescents with attention deficit hyperactivity disorder. Neurosci. Lett. 400, 39–43.

Tzourio-Mazoyer, N., Landeau, B., Papathanassiou, D., Crivello, F., Etard, O., Delcroix, N., Mazoyer, B., Joliot, M., 2002. Automated anatomical labeling of activations in SPM Using a macroscopic anatomical parcellation of the MNI MRI single-subject brain. NeuroImage 15, 273–289.

Uddin, L.Q., Kelly, A.M.C., Biswal, B.B., Margulies, D.S., Shehzad, Z., Shaw, D., Ghaffari, M., Rotrosen, J., Adler, L.A., Castellanos, F.X., Milham, M.P., 2008. Network homogeneity reveals decreased integrity of default-mode network in ADHD. J. Neurosci. Methods 169, 249–254.

Vaidya, C.J., Austin, G., Kirkorian, G., Ridlehuber, H.W., Desmond, J.E., Glover, G.H., Gabrieli, J.D.E., 1998. Selective effects of methylphenidate in attention deficit hyperactivity disorder: a functional magnetic resonance study. Proc. Natl Acad. Sci. U. S. A. 95, 14494–14499.

Valera, E.M., Faraone, S.V., Murray, K.E., Seidman, L.J., 2007. Meta-analysis of structural imaging findings in Attention-Deficit/Hyperactivity Disorder. Biol. Psychiatry 61, 1361–1369.

Wang, J., Jiang, T., Cao, Q., Wang, Y., 2007. Characterizing anatomic differences in boys with Attention-Deficit/Hyperactivity Disorder with the use of deformation-based morphometry. Am. J. Neuroradiol. 28, 543–547.

Wellington, T.M., Semrud-Clikeman, M., Gregory, A.L., Murphy, J.M., Lancaster, J.L., 2006. Magnetic resonance imaging volumetric analysis of the putamen in children with ADHD combined type versus control. J. Atten. Disord. 10, 171–180.

Yang, L., Wang, Y.F., Qian, Q.J., Gu, B.M., 2001. Primary exploration of the clinical subtypes of attention deficit hyperactivity disorder in Chinese children (in Chinese). Chin. J. Psychiatry 34, 204–207.